

Article

An Automatic System for Remote Monitoring of *Bactrocera dorsalis* Population

Shao-Ping Chen ^{1,2,†}, Shi-Lei Zhu ^{1,2,†}, Rong-Zhou Qiu ^{1,2}, Mei-Xiang Chi ^{1,2}, Yan Shi ^{1,2}, Jia-Xiong Chen ^{1,2}, Yong Liang ³ and Jian Zhao ^{3,*} 

¹ Institute of Plant Protection, Fujian Academy of Agricultural Sciences, Fuzhou 350013, China; fafucsp@163.com (S.-P.C.); 52302031021@fafu.edu.cn (S.-L.Z.); qurz@faas.cn (R.-Z.Q.); cmx895619@163.com (M.-X.C.); shiyancy@163.com (Y.S.); 12402113001@fafu.edu.cn (J.-X.C.)

² Fujian Key Laboratory for Monitoring and Integrated Management of Crop Pests, Fujian Engineering Research Center for Green Pest Management, Fuzhou 350013, China

³ Institute of Digital Agriculture, Fujian Academy of Agricultural Sciences, Fuzhou 350013, China; tiger310@163.com

* Correspondence: zhaojian@faas.cn

† These authors contributed equally to this work.

Abstract

Bactrocera dorsalis (Hendel, 1912) is a highly destructive pest affecting fruits and vegetables, making population monitoring essential for farmers to implement timely control measures. In recent years, although automatic monitoring systems for *B. dorsalis* have been introduced, challenges such as limited accuracy, difficulty in accurately identifying the target pest using infrared interruption sensors alone, and high labor requirements persist. This study presents an automatic monitoring system consisting of intelligent bait equipment (IBE), an advanced detection model based on YOLOv8, and an online monitoring platform. The developed IBE is equipped with cameras, attractant-based lures, and an automatic removal mechanism for *B. dorsalis*. Field tests demonstrated the IBE exhibited an attractiveness to *B. dorsalis* comparable to conventional traps, achieved a near-perfect cleaning efficiency (~100%), and maintained a reliable wireless transmission system. The YOLOv8l-based automatic pest detection model outperformed other YOLOv8 variants (n, s, m, x), achieving the highest precision (95.17%), recall (94.15%) and F1 score (94.66%), underscoring its effectiveness in pest detection. Further analysis of the impact of *B. dorsalis* density on YOLOv8l's detection performance revealed a decline in accuracy as density increased; however, even at high densities, the model maintained a strong F1 score of 93.36%, demonstrating robustness. Finally, the automatic pest detection model was integrated into 'YunShanPu', an online platform for real-time pest monitoring. The proposed method has demonstrated promising performance in the automatic identification and counting of *B. dorsalis* and has potential for monitoring *B. dorsalis* populations continuously, providing early warning and forecasting for integrated pest management.



Academic Editor: Pei Wang

Received: 11 October 2025

Revised: 14 November 2025

Accepted: 18 November 2025

Published: 19 November 2025

Citation: Chen, S.-P.; Zhu, S.-L.; Qiu, R.-Z.; Chi, M.-X.; Shi, Y.; Chen, J.-X.; Liang, Y.; Zhao, J. An Automatic System for Remote Monitoring of *Bactrocera dorsalis* Population. *Agriculture* **2025**, *15*, 2391.

<https://doi.org/10.3390/agriculture15222391>

Copyright: © 2025 by the authors. Licensee MDPI, Basel, Switzerland. This article is an open access article distributed under the terms and conditions of the Creative Commons Attribution (CC BY) license (<https://creativecommons.org/licenses/by/4.0/>).

Keywords: *Bactrocera dorsalis*; YOLO; automatic detection; intelligent bait equipment

1. Introduction

Bactrocera dorsalis (Hendel, 1912) (oriental fruit fly, Diptera: Tephritidae) is a globally significant quarantine pest that infests over 250 host plant species, including major fruit crops such as orange, guava, mango, carambola, and papaya [1–3]. The pest has spread to almost all regions worldwide in recent decades, emerging as a major concern due to

its severe impact on global fruit and vegetable production [4,5]. Adults oviposit beneath the fruit surface, and larvae develop inside before leaving the fruit to pupate in the soil, remaining protected from insecticide treatments; thus, adult flies are the primary target for field control [6–9]. The primary control strategy for *B. dorsalis* relies on chemical pesticides; however, studies indicate that prolonged and frequent insecticide applications have resulted in a high level of resistance [10–12]. Current integrated pest management (IPM) strategies, which combine biological, chemical, physical, and other control methods, offer a sustainable and effective solution for controlling *B. dorsalis* [3,4].

Monitoring and early warning of pests play a crucial role in IPM by enabling timely interventions to reduce population outbreaks, minimize crop damage, and optimize control strategies [13–16]. Traditionally, *B. dorsalis* populations are monitored by placing yellow plastic traps containing a mixture of methyl eugenol (ME) and insecticide [2,4,17]. Manual field visits and counting are labor-intensive, expensive, time-consuming, and prone to error [2,18,19]. Given these limitations, the development of automated monitoring systems for *B. dorsalis* is crucial for improving accuracy, reducing labor costs, and enabling real-time pest surveillance, ultimately contributing to more effective and sustainable pest management.

Numerous studies have explored the automatic monitoring of *B. dorsalis*, with systems utilizing ME-baited traps equipped with infrared diodes and photoelectric sensors based on wireless communication technology, enabling trap count monitoring but cannot identify species [13,20]. To address this limitation, Tariq et al. [21] developed a smart trap with image capture capabilities, integrating with a mobile application for real-time monitoring and achieving a diagnostic accuracy of 85%. Additionally, Diller et al. [22] introduced a McPhail-type electronic trap based on deep learning for fruit flies, including *B. dorsalis*, attaining an average precision (AP) of 93.53%; however, this design relied on yellow sticky traps. Despite these advancements, challenges remain, such as limited detection accuracy and the high cost associated with replacing yellow sticky traps [21,22].

In this study, the primary objective was to develop a low-cost, durable, and reliable system, capable of operating under field conditions for extended periods without human intervention. To achieve this, a self-cleaning intelligent bait equipment (IBE) integrating cameras and attractants was developed first. The proposed IBE is capable of capturing *B. dorsalis*, imaging them, and subsequently removing them automatically. The effectiveness of IBE in attracting *B. dorsalis* and its cleaning efficiency were evaluated through an 8-day field test. Following this, an image dataset was collected from IBEs deployed in the field for nearly 1 year and utilized to develop an intelligent recognition model for *B. dorsalis* based on the YOLOv8 architecture. The impact of pest density on the model's performance was analyzed. Finally, an online monitoring platform was developed to support practical implementation, and the system was validated through an additional four months of field testing.

2. Materials and Methods

2.1. The Design of Intelligent Bait Equipment

The intelligent bait equipment (IBE) developed in this study consists of a pest trapping device, an image-taking chamber and a control box (Figure 1). Specifically, a pest entrance (12 mm in diameter) is designed according to the insect's size. A circular power grid with an automatic cleaning function is installed in the middle of the trapping device, and pheromone lure placement point is arranged in the center of the power grid. Furthermore, a lid is arranged directly above the trapping device to prevent rainwater from entering the trap. The bottom of the trapping device features an anti-climbing funnel leading to the image-taking room. A built-in camera (1800 × 1350 pixels) is located above the

image-taking room, facing the center of the white detection board (136 mm in diameter). To prevent environmental dust from affecting the images, the camera is equipped with a flip lens cover. A circular LED light panel (122 mm in diameter), comprising 17 beads (1026 LED, white light), is embedded above the image-taking room to ensure even illumination and consistent image quality. The white board is located at the bottom of the image-taking room and has a flipping function. Beneath the white board is a pest collection bin. A fan (9GL1212V1J03, SanAce120L, Shenzhen, China) is installed below the pest collection bin to remove dust, ensuring the quality of images captured by the camera. The control box includes a lithium battery storing electricity for the solar panel (560 mm × 530 mm), an image storage and transmission module (8 GB memory card and 4G module card), and a multifunction controller responsible for timing lights, camera shooting, opening fans, and operating the image storage and transmission module. To prevent airflow from disturbing insect specimens during imaging, the image capture process was programmed to occur before fan activation. The IBE employs a weatherproof shell to ensure stable operation outdoors.

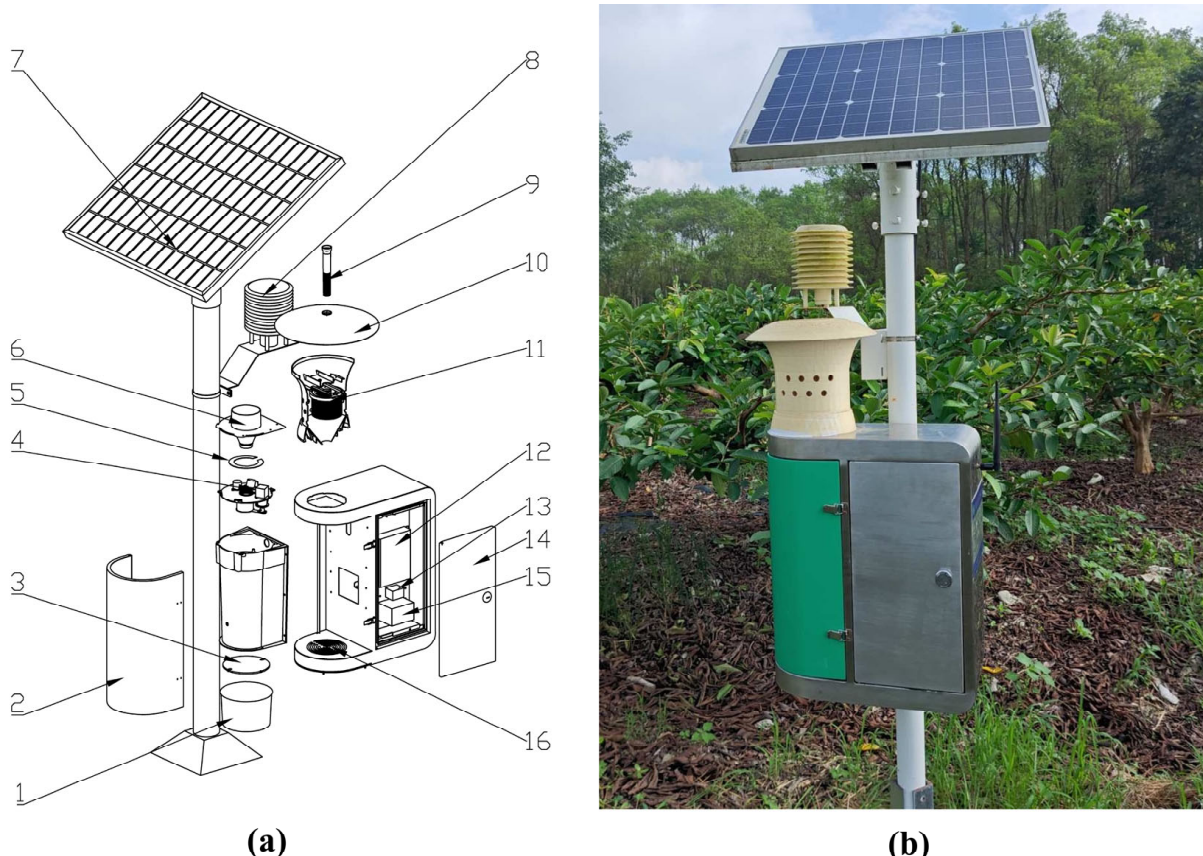


Figure 1. Intelligent bait equipment for automatic in-trap *Bactrocera dorsalis* detection. (a), exploded views of the intelligent bait equipment. 1, pest collection bin; 2, shell; 3, white detection board; 4, camera; 5, circular LED light panel; 6, anti-climbing funnel; 7, solar panel and the bracket; 8, temperature and humidity sensor; 9, attractant pheromone placement point; 10, lid; 11, circular power grid; 12, image storage and transmission module; 13, multifunction controller; 14, shell; 15, lithium battery; 16, fan. (b), Physical image of the intelligent bait equipment.

The main steps for the IBE operation (Figure 2) are summarized as follows:

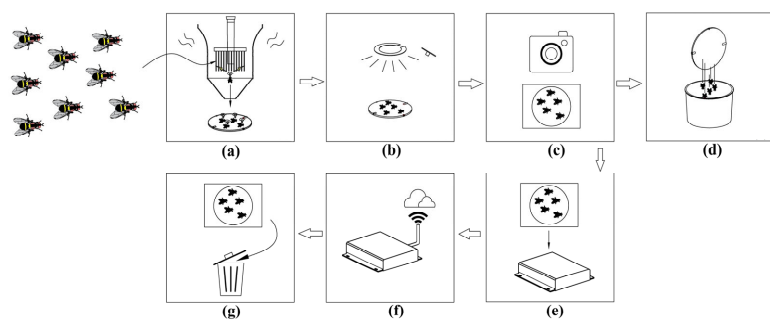


Figure 2. Diagram illustrating the operation processes of intelligent bait equipment. (a), pest attraction and electrocution; (b), turn on the light; (c), take images; (d), pest removing automatically; (e), save images locally; (f), send images to Alibaba Cloud Object Storage Service; (g), delete the local backup.

The target pests enter the trap and are electrocuted and fall into the white detection board when they approach the attractant. At the preset shooting time, the multifunction controller first turns on the LED light and then controls the camera to take images of the pests falling on the detection board. After the shooting is completed, the multifunction controller flips the white detection board 180° and pests fall into the pest collection bin. The image is stored in the memory card and subsequently transmitted to Alibaba Cloud Object Storage Service (OSS) through the 4G module. The image is then deleted from the memory card.

2.2. Short-Term Field Test of Intelligent Bait Equipment

Three IBEs for *B. dorsalis* were installed in guava orchards on Lüfu Farm (24.6229° N, 117.7644° E), Changtai, Zhangzhou City, Fujian Province, China, starting from 16 August 2023 (Figure 3). The IBE automatically takes photos twice a day at 12:00 and 21:00. The attractiveness of the IBEs to *B. dorsalis* was compared with that of conventional traps (height, 220 mm × diameter, 96 mm; Enjoy Agricultural Technology Co., Ltd., Zhangzhou, China) over 8 days (17–24 August 2023). The entomologist, a recognized expert in the field, maintained both conventional traps and IBEs, collecting data on the numbers of *B. dorsalis* that were attracted and trapped. The entomologist also inspected images uploaded by the IBEs to the Alibaba Cloud Object Storage Service daily. ME was used as an attractant for *B. dorsalis* males. It is worth noting that the identification of *B. dorsalis* was confirmed not only by external morphological characteristics but also through molecular methods.



Figure 3. Intelligent bait equipment for *Bactrocera dorsalis* installed in guava orchards. a, Intelligent bait equipment 1; b, conventional trap 1; c, Intelligent bait equipment 2; d, conventional trap 2; e, Intelligent bait equipment 3; f, conventional trap 3.

2.3. Automatic Pest Counting

2.3.1. Image Dataset Construction and Annotation

A total of 852 images were collected from field using IBEs over nearly one year (24 August 2023–31 August 2024) and were randomly separated into a training set and a validation set at a 4:1 ratio (Table 1). To enhance model performance, deep learning approaches require large datasets, and image data augmentation is a widely used technique for dataset expansion [23,24]. Therefore, the training set images were augmented 12-fold using various augmentation techniques, including flipping, rotation, brightness adjustment, contrast adjustment, Gaussian blur, and noise addition. A further 203 images collected from the field via IBEs were utilized exclusively as a testing set. The datasets included simple images of a few *B. dorsalis* without body stacking and complex images of many *B. dorsalis*, in which body stacking and/or interference from other insects may occur (Figure 4). Such diverse conditions provided a solid basis for developing a model suitable for real field environments. The resolution of the images was 640×640 pixels.

Table 1. Statistics of the constructed datasets.

Datasets	Number of Images	Number of Labels
Training set	682	12,472
Validation set	170	3415
Test set	203	7148

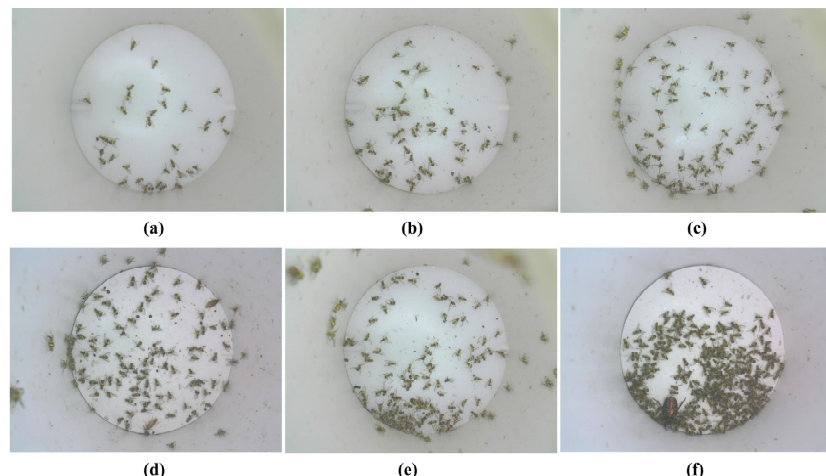


Figure 4. Examples of *Bactrocera dorsalis* images captured by the intelligent bait equipment. (a–c), Simple images with few *B. dorsalis* without body stacking captured in the field; (d–f), complex images with many *B. dorsalis*, in which body stacking and/or interference from other insects may be captured in the field.

B. dorsalis individuals were identified and labeled by an entomologist using the custom software ‘HyperSpider LabelTool’ (Version 1.0) [25]. The specific labeling information can be found in Table 1. The bounding box was minimized to cover only the target pest, specifically including the bodies and wings of *B. dorsalis*, while not necessarily encompassing the antennae and legs [26]. The annotation files were saved in TXT format, with identical names used as their corresponding images.

2.3.2. Automatic Pest Counting Models Based on YOLOv8

The YOLO series is a widely recognized single-stage object detection algorithm known for its fast detection speeds, real-time performance, efficiency, and flexibility, achieving significant advancements in object detection [25,27–30]. YOLOv8 offers models in various

sizes (n/s/m/l/x scales) to meet diverse scene requirements, performs well in real-world agricultural pest detection tasks, showing high accuracy and robustness under field conditions [31]. In this study, an intelligent recognition model for *B. dorsalis* was developed based on the YOLOv8. Model performance was evaluated via linear regression between automatically and manually counted *B. dorsalis* in each image. The optimal model was selected to further analyze the impact of pest density on detection performance. For this analysis, the test set was categorized into three subsets: low, medium, and high density (Table 2).

Table 2. Division of the test set into low-, medium-, and high-density subsets.

Density	Number of Images	Number of Labels	Number of Labels Per Image
Low	69	438	$n < 15$
Medium	66	1732	$15 \leq n \leq 40$
High	68	4978	$n > 40$

All experiments were executed on a system with Intel I7-12700K@3.60 GHz-core processor, 16 GB NVIDIA RTX 4070 Ti Super GPU, and 64 GB of memory. The software environment comprised Pytorch 2.5.1, CUDA 12.6 and torch-vision 0.20.1. All models were optimized using stochastic gradient descent (SGD) with a fixed learning rate of 0.01, a fixed batch size of 16, a fixed number of epochs of 200, a fixed momentum of 0.937, a confidence level threshold greater than 0.4, and an intersection over union (IoU) greater than 0.5.

2.3.3. Model Evaluation

The precision (P), recall (R), and F1 score were selected to evaluate the model. Hossin and Sulaiman described these evaluation metrics in detail [32]. Briefly, precision measures the proportion of positive objects assigned correctly. In other words, precision quantifies the correct positive predictions. In contrast to precision, recall estimates the ability of a model to label all positive objects. This metric indicates how many positive objects the model correctly identifies as positive. The F1 score is simply a measure that aims to weight the importance of precision and recall. Higher F1 scores indicate better model performance. The precision, recall, and F1 score are computed as follows:

$$\text{Precision (P)} = \frac{\text{TP}}{\text{TP} + \text{FP}} \quad \text{Recall (R)} = \frac{\text{TP}}{\text{TP} + \text{FN}} \quad \text{F1 scores (F1)} = \frac{2\text{PRP} + R}{2\text{PRP} + R + \text{FN}} \quad (1)$$

where TP, FP and FN represent the numbers of true positive, false positive and false negative outcomes detected by the model, respectively.

2.4. Long-Term Field Deployment of Integrated Pest Monitoring System

To facilitate the practical implementation of the model, a platform called 'YunShanPu' (Version 1.0) was developed based on a Browser/Server Architecture. The platform achieves seamless integration of hardware and software through a well-defined workflow (Figure 5). In brief, the platform integrates hardware and software, enabling real-time monitoring of IBEs, receiving uploaded images, reviewing images by date, and performing automatic pest detection w the trained model. The system has been operationally tested in guava orchards since 1 September 2024.

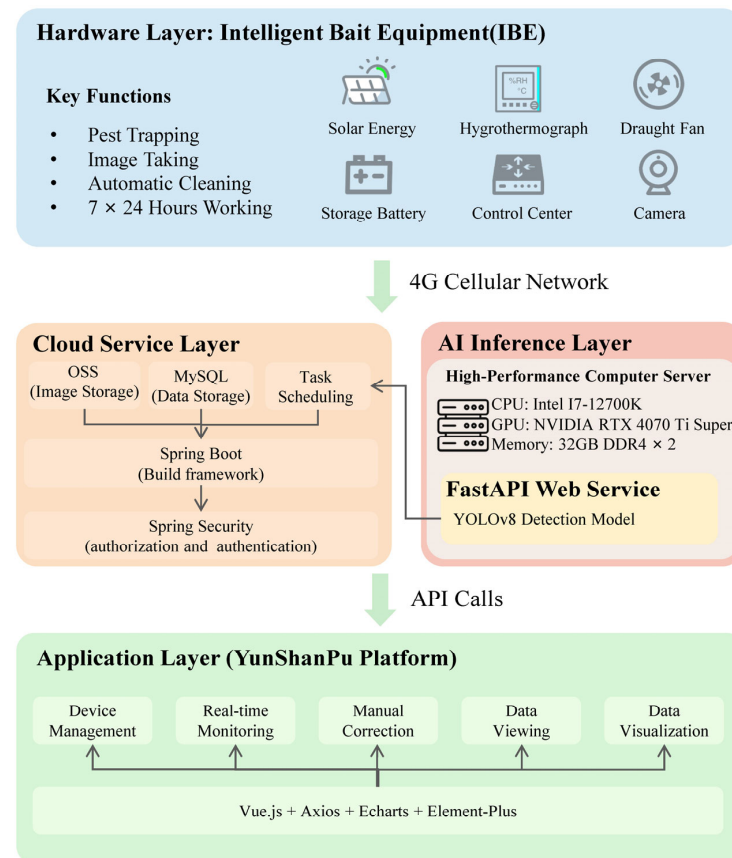


Figure 5. System architecture of ‘YunShanPu’ platform.

3. Results

3.1. Intelligent Bait Equipment Function and Attractiveness of *B. dorsalis*

The study results indicated that the developed IBE demonstrated an attractiveness to *B. dorsalis* comparable to conventional traps, with both methods capturing a similar number of flies ($t = 1.680$, $df = 7$, $P = 0.137$; Figure 6a). The IBEs achieved a cleaning efficiency close to 100% (Figure 6b), highlighting their stable cleaning capacity. The average image upload time was approximately 2 s, with no significant differences among the three IBEs ($\chi^2 = 1.044$, $df = 2$, $P = 0.593$; Figure 6c), indicating the reliability of the wireless transmission system. Additionally, throughout the field deployment, the batteries remained functional without the need for replacement, and no electronic malfunctions were recorded.

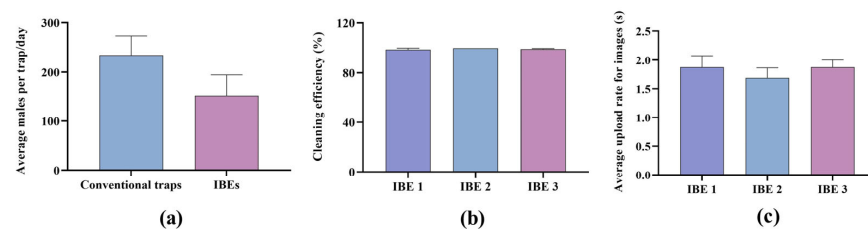


Figure 6. Field performance of intelligent bait equipment. (a), average number of *B. dorsalis* captured per trap per day with both intelligent bait equipment and conventional traps; (b), cleaning efficiency; (c), average rate of image uploading to Alibaba Cloud Object Storage Service. All field performance tests were conducted over an 8-day period using three IBEs. A paired *t*-test was performed to compare the attractiveness between the IBE and conventional traps, while the Kruskal–Wallis test was conducted to assess whether significant differences existed among the three IBEs in average image upload time.

3.2. The Pest Detection Results Based on YOLOv8 Models

The YOLOv8-based automatic pest detection models exhibited comparable precision, all exceeding 94.68%, with YOLOv8l achieving the highest precision of 95.17% (Table 3). In terms of recall, YOLOv8n showed the lowest performance, while YOLOv8l achieved the highest recall of 94.15% (Table 3). Overall, the YOLOv8l-based automatic pest detection model outperformed other YOLOv8 variants, achieving the highest precision, recall and F1 score.

Table 3. Comparison of detecting results for several series models of YOLOv8.

Models	P	R	F1	FPS
YOLOv8n	94.68%	92.21%	93.43%	224
YOLOv8s	95.03%	93.10%	94.06%	215
YOLOv8m	95.04%	93.85%	94.44%	151
YOLOv8l	95.17%	94.15%	94.66%	90
YOLOv8x	94.69%	92.87%	93.77%	61

A comparative analysis between model-based automatic counting and manual counting of *B. dorsalis* in each image was performed. The linear regression analysis presented in Figure 7 suggested that the YOLOv8l model achieved a slightly superior correlation ($R^2 = 0.9959$) compared to other YOLOv8 variants, indicating that its detection results were most closely aligned with manual counting. Additionally, the histogram of counting error showed that the counting errors for YOLOv8l were predominantly concentrated within ± 10 , and it had the largest number of correct detection images (Figure 7).

3.3. Effect of *B. dorsalis* Densities on YOLOv8l Model Detection Performance

To further assess the YOLOv8l model's performance at different population densities, we divided the test set into three subsets: low, medium, and high density. As population density increased, the model's detection precision, recall and F1 score all decreased, with recall dropping by 6.54% from low to high density (Table 4).

Table 4. Effect of *Bactrocera dorsalis* densities on YOLOv8l model detection performance.

Density	P	R	F1
Low ($n < 15$)	97.94%	99.06%	98.50%
Medium ($15 \leq n \leq 40$)	96.86%	98.10%	97.48%
High ($n > 40$)	94.21%	92.52%	93.36%

The model maintained good detection performance when individuals were sparsely distributed, even under high-density conditions (Figure 8). However, when individuals were highly overlapping or stacked, the model often failed to distinguish them correctly, resulting in missed or merged detections and reduced counting accuracy (Figure 9). These errors mainly occurred when individuals were partially occluded or formed dense clusters with unclear body boundaries, which limited YOLOv8l's ability to separate adjacent targets under high-density conditions.

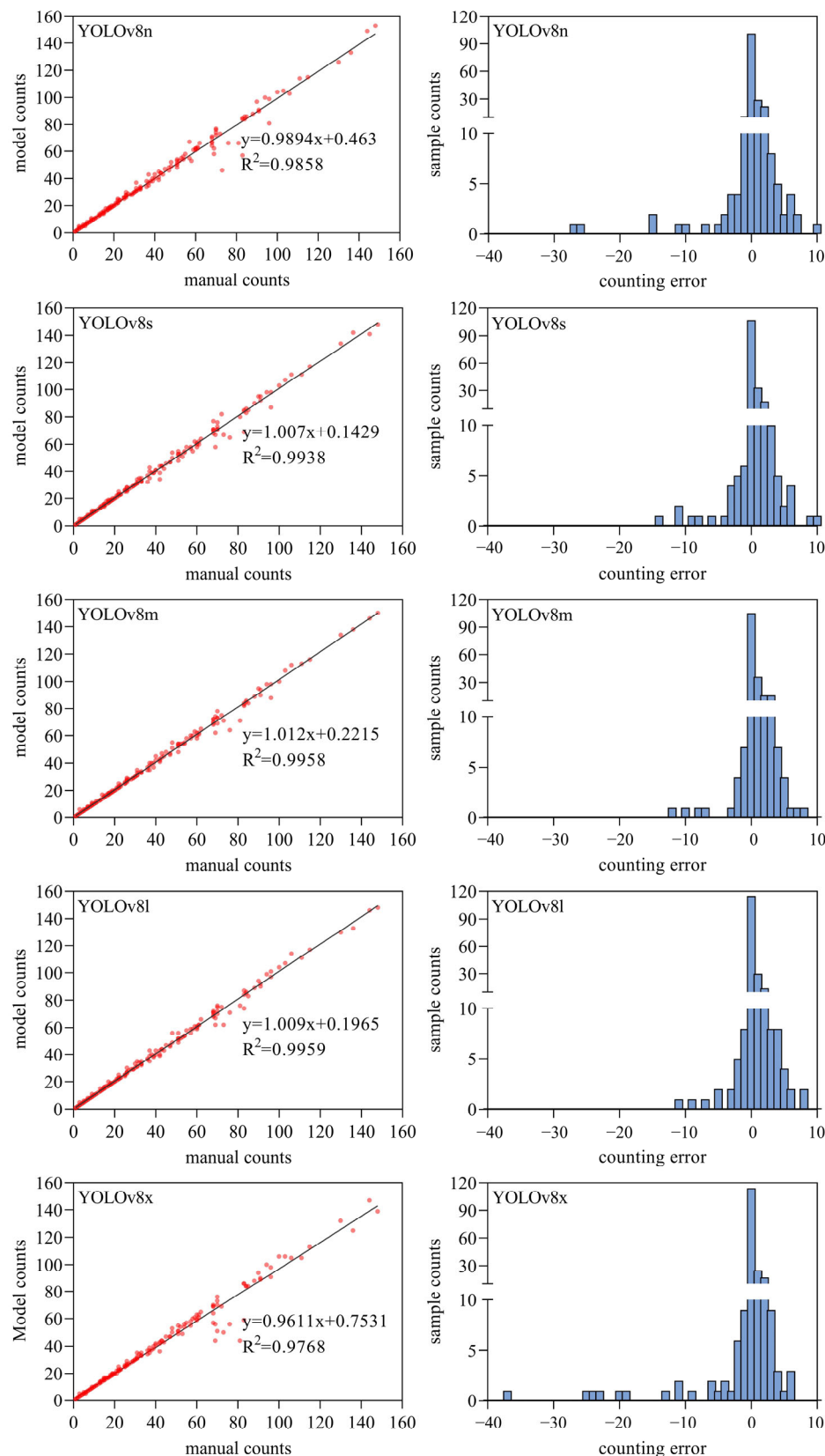


Figure 7. Plot of the counting test results of the YOLOv8 models. The left figure is a plot of the linear regression results between the manual counts and the model counts derived from image samples. The right figure is a histogram of the counting error, where the x-axis represents the counting error of the model, and the y-axis represents the number of image samples.

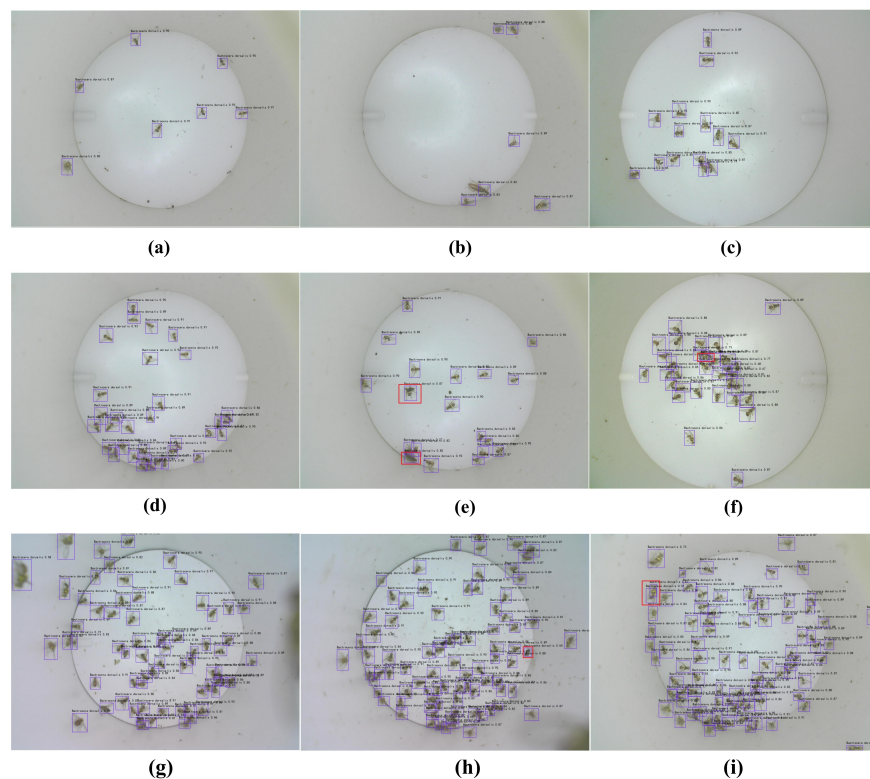


Figure 8. Example of detection results for the YOLOv8l model at varying *Bactrocera dorsalis* densities. (a–c), low density; (d–f), medium density; (g–i), high density. The red rectangular box represents incorrect detection or missed detection.

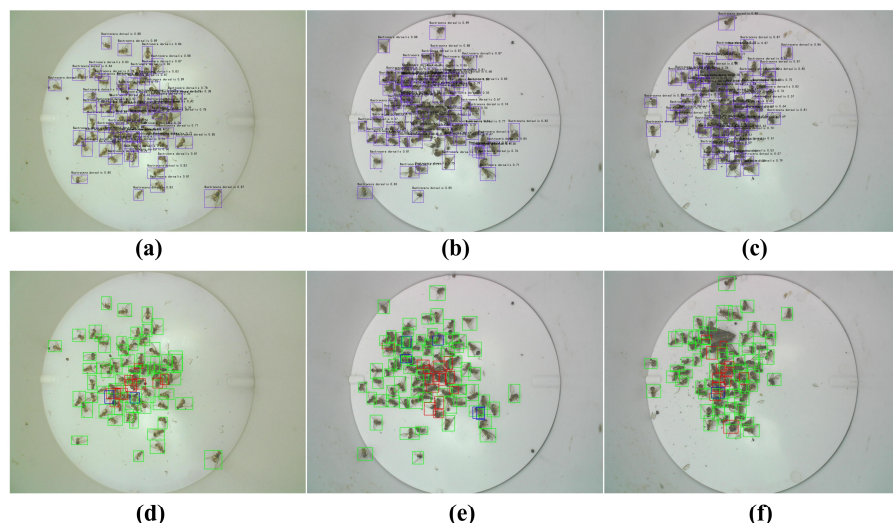


Figure 9. Example of detection results for the YOLOv8l model at high *Bactrocera dorsalis* density. (a–c), model detection results; (d–f), correction of model detection results based on entomologist labeling. The red rectangular box represents missed detection, and the blue rectangular box represents incorrect detection.

3.4. Pest Online Remote Monitoring

To facilitate the practical implementation of the automatic pest counting model, a platform called ‘YunShanPu’ was developed in our study. Through the web-based software, users can select specific IBEs to check pest counts (Figure 10a). The page displays the pest count directly, and users can also view the corresponding images for optional manual validation (Figure 10b).

(a)

ID	Time	Flag	Result	Count	Correct Num	Used Model	Upload Time	Image	Operation
1	2024-10-23 21:09:08	identified	Bactrocera dorsalis	5	edit	YOLOv8l	2024-10-23 21:12:41	check	approved
2	2024-10-23 12:08:29	identified	Bactrocera dorsalis	4	edit	YOLOv8l	2024-10-23 12:16:19	check	approved
3	2024-10-22 21:09:58	identified	Bactrocera dorsalis	8	edit	YOLOv8l	2024-10-22 21:11:39	check	approved
4	2024-10-22 12:09:31	identified	Bactrocera dorsalis	5	edit	YOLOv8l	2024-10-22 12:16:01	check	approved
5	2024-10-21 21:09:01	identified	Bactrocera dorsalis	6	edit	YOLOv8l	2024-10-21 21:11:35	check	approved
6	2024-10-21 12:09:17	identified	Bactrocera dorsalis	12	edit	YOLOv8l	2024-10-21 12:13:33	check	approved
7	2024-10-20 21:08:41	identified	Bactrocera dorsalis	10	edit	YOLOv8l	2024-10-20 21:11:58	check	approved
8	2024-10-20 12:09:12	identified	Bactrocera dorsalis	6	edit	YOLOv8l	2024-10-20 12:40:01	check	approved
9	2024-10-19 21:09:37	identified	Bactrocera dorsalis	2	edit	YOLOv8l	2024-10-19 21:12:10	check	approved
10	2024-10-19 12:08:57	identified	Bactrocera dorsalis	18	edit	YOLOv8l	2024-10-19 12:11:30	check	approved

1-10 total 10 < 1 > 10/page ✓

(b)

Figure 10. The software interface of ‘YunShanPu’. (a), home page; (b), pest diagnosis result display interface.

Additionally, users can select images from a specific date to review the pest count. Data from three IBEs collected between 1 September 2024, and 31 December 2024, showed similar pest occurrence trends across the three IBEs, with a peak period from early September to mid-October (Figure 11). When the *B. dorsalis* count did not exceed 50, the model’s counts closely matched the manual counts (Figure 11). These results indicated that our system can reliably capture pest occurrence trends, enabling growers to detect surges early and take preventive action. Moreover, the system operated continuously from September to December, consistently recording population dynamics in real orchards, demonstrating the long-term stability required for agricultural deployment.

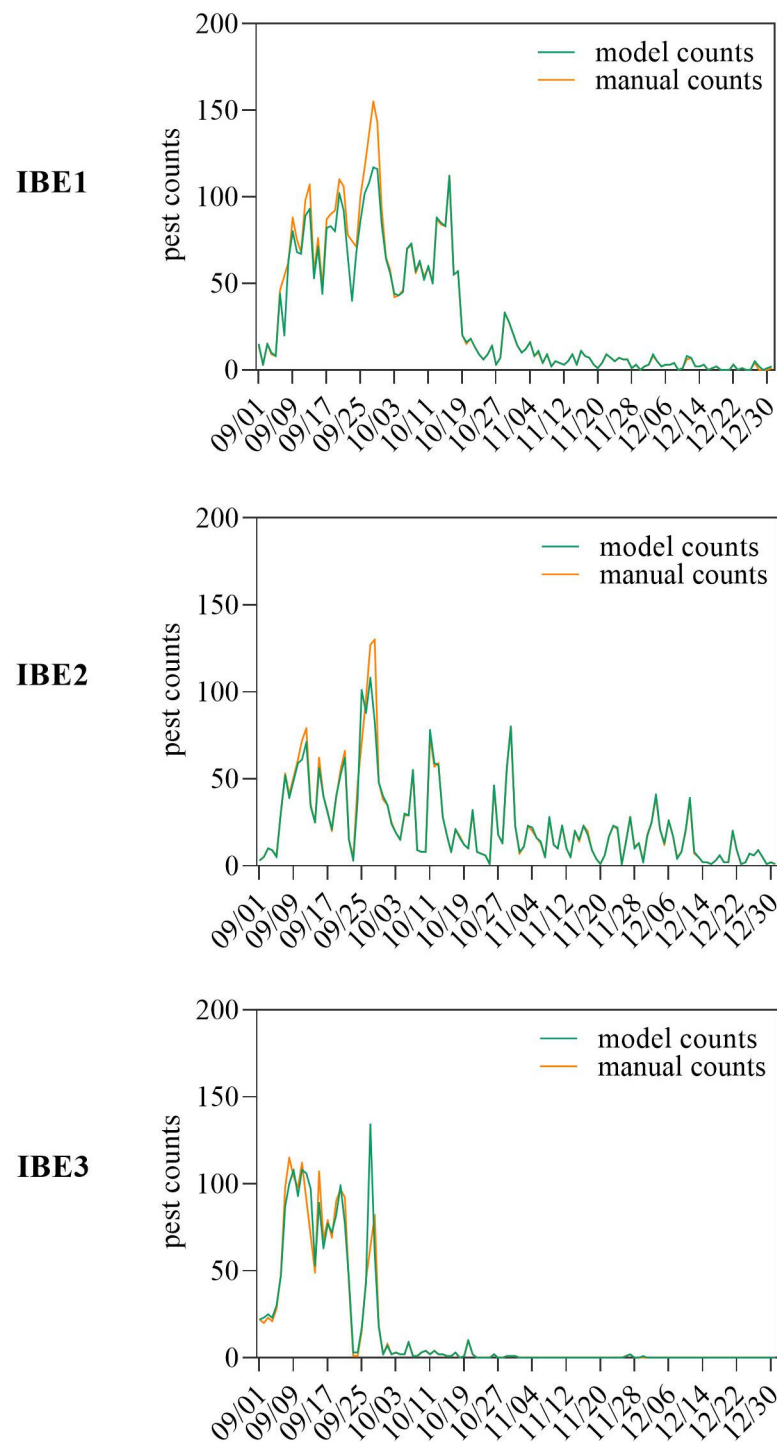


Figure 11. Comparison of *Bactrocera dorsalis* counts from model detection and manual validation (1 September 2024–31 December 2024).

4. Discussion

In this study, an IBE integrated with a YOLOv8-based automatic pest detection model and the 'YunShanPu' online monitoring platform was developed for remote surveillance of *B. dorsalis* populations in guava orchards. First, an IBE for automatic in-trap *B. dorsalis* detection was developed. An 8-day field test showed the IBE exhibited attractiveness to *B. dorsalis* comparable to conventional traps, while capturing clear, high-quality images of target pests against a clean, uniform background, automatically removing individuals after imaging, and transmitting data in real time. This brief testing period provided a

preliminary evaluation of the IBE's functionality under field conditions. However, the relatively short duration of the test limited the number of observations, which may have contributed to larger variation and reduced statistical power. Future studies will conduct monthly comparisons between IBEs and conventional traps, aligned with the methyl eugenol replacement cycle, to robustly evaluate the IBE's trapping efficiency. Overall, our developed IBE meets the suggested requirements for developing a camera-equipped automatic trap proposed by Preti et al. [33], including a reliable power supply with low power consumption, a waterproof and compact structure that optimally accommodates all the required electronic components, an appropriate trap with effective attractants, a built-in camera that can capture high-quality images, and a good wireless transmission system. In addition, a white detection board was used in our equipment instead of a sticky board. Compared with sticky boards based electronic traps [22], the standard white detection board utilized in our equipment requires less intensive human work because it can flip over automatically for *B. dorsalis* removal.

The YOLOv8-based automatic pest detection models demonstrated strong performance, achieving F1 scores exceeding 93.43%. YOLOv8 has made notable advancements in object detection, including applications in tobacco and crop pest monitoring [28,34,35]. Another contributing factor to the model's effectiveness is the image dataset, which was collected over nearly a year from guava orchards, accurately reflecting actual field conditions of *B. dorsalis* attraction to IBEs in the field. Numerous studies have highlighted that image datasets closely aligned with actual field conditions hold significant potential for practical applications [18,22,36–38]. The YOLOv8l-based automatic pest detection model was selected because it outperformed other YOLOv8 variants, achieving the highest precision, recall and F1 score. In practical field monitoring, even slight improvements in accuracy are valuable, as they can effectively reduce false positives and missed detections that may compromise the reliability of pest population assessments. Further analysis showed that detection accuracy declined as *B. dorsalis* density increased, likely due to increased body overlap at higher densities. The negative impact of severe insect overlap on recognition performance remains a significant challenge in pest detection research [29,30]. To address this issue, we plan to optimize the model through algorithmic improvements, such as incorporating an appropriate attention mechanism to strengthen the model's ability to localize densely packed insects [34,35,39], introducing repulsion loss to enhance spatial separation between predicted bounding boxes and reduce merging errors [40], and implementing copy-paste data augmentation to increase the proportion of high-density samples in training [41], thereby improving model generalization under overlapping insect scenarios. Additionally, we intend to utilize the automatic cleaning function of IBEs to collect image data multiple times per day in future studies, further enhancing detection reliability.

Current research on agricultural pest detection primarily focuses on improving detection algorithms [27–30,34,35]. However, since the recognition accuracy of our model is sufficient for field application, no further algorithm improvement experiments were conducted in this study. Compared with previously reported automatic monitoring systems for *B. dorsalis*, our system demonstrates several distinctive advantages that enhance its field applicability. Tariq et al. [21] developed a mobile-integrated smart trap achieving 85% diagnostic accuracy; however, this limited accuracy may constrain its reliability for pest management decisions. Diller et al. [22] proposed a McPhail-type deep learning trap, attaining an average precision of 93.53%, but it relied on yellow sticky traps, which are costly and labor-intensive to replace. In contrast, our IBE captures images against a clean, featureless background and automatically removes flies after imaging, eliminating the need for sticky materials and reducing operational costs and maintenance (the IBE only requires inspection when replacing the ME). Moreover, the IBE operates using solar-charged batter-

ies that required no replacement during the entire monitoring period, demonstrating high energy efficiency and minimal maintenance. The IBE incurs almost no daily operational cost, as it functions autonomously and only requires periodic inspection to replace the ME attractant when necessary.

The integration of IBEs with a high-performing YOLOv8l-based detection model and the “YunShanPu” platform enables real-time remote access to pest data directly from orchards, facilitating timely decision-making such as optimizing pesticide application schedules based on population trends. This can improve control efficacy and reduce environmental impact. The IBEs accurately identified peaks in *B. dorsalis* occurrence, with the highest activity from early September to mid-October, demonstrating the system’s ability to provide early warning of population surges and allowing growers to take action before economic damage occurs. In addition, the automated nature of the IBE and platform substantially reduces labor by eliminating frequent manual trap inspections while ensuring continuous and reliable data collection with minimal human intervention. Overall, the system reduces labor requirements and provides timely, reliable information for initiating early-warning responses to sudden population surges, thereby supporting data-driven IPM strategies.

Although the proposed automatic monitoring system for *B. dorsalis* performed well under field conditions, additional research is required to translate its outputs into actionable agricultural decisions. A key next step is to establish quantitative relationships among IBE trap catches, actual population density, and economic thresholds, which are fundamental to precise pest management. To support this, future work will integrate environmental variables (e.g., temperature, humidity), pesticide application records, and entomologist-surveyed population data. A multi-year dataset incorporating these factors will be compiled to enable the development of predictive models and decision-support tools for precision agriculture, thereby enhancing early warning capabilities and optimizing control strategies.

5. Conclusions

The proposed system integrates an intelligent bait equipment (IBE), a deep learning-based pest detection model, and the “YunShanPu” online platform for real-time pest monitoring of *B. dorsalis*. The IBE enables automated image acquisition against a clean and uniform background and automatic removal of target insects, ensuring high-quality image data for accurate detection. The key advantage of this system is its ability to reduce labor requirements while delivering timely, accurate, and reliable data directly from orchards, demonstrating strong potential for early pest warning in the event of sudden population surges.

Overall, this study established a technical foundation for data-driven and intelligent pest management. In future research, we plan to expand multi-year datasets that incorporate environmental and agronomic variables to strengthen correlations between trap catches and field pest population dynamics, and to refine early warning and intervention thresholds for sustainable integrated pest management.

Author Contributions: Conceptualization, J.Z. and S.-P.C.; methodology, R.-Z.Q. and S.-P.C.; software, S.-L.Z.; validation, M.-X.C., Y.S. and J.-X.C.; formal analysis, R.-Z.Q. and S.-L.Z.; investigation, Y.L.; data curation, S.-P.C., S.-L.Z. and Y.L.; writing—original draft preparation, S.-P.C. and S.-L.Z.; writing—review and editing, J.Z.; visualization, M.-X.C., Y.S. and J.-X.C.; supervision, R.-Z.Q.; project administration, S.-P.C.; funding acquisition, J.Z. All authors have read and agreed to the published version of the manuscript.

Funding: This research was funded by the Basic Research Special Foundation of the Public Research Institutes of Fujian Province, grant number 2022R1024005.

Data Availability Statement: The data that support the findings of this study are available from the corresponding author upon reasonable request.

Conflicts of Interest: The authors declare no conflicts of interest.

References

1. Jaleel, W.; Tao, X.; Wang, D.; Lu, L.; He, Y. Using two-sex life table traits to assess the fruit preference and fitness of *Bactrocera dorsalis* (Diptera: Tephritidae). *J. Econ. Entomol.* **2018**, *111*, 2936–2945. [\[CrossRef\]](#) [\[PubMed\]](#)
2. Lello, F.; Dida, M.; Mkiramweni, M.; Matiko, J.; Akol, R.; Nsabagwa, M.; Katumba, A. Fruit fly automatic detection and monitoring techniques: A review. *Smart Agric. Technol.* **2023**, *5*, 100294. [\[CrossRef\]](#)
3. Jaffar, S.; Rizvi, S.A.H.; Lu, Y. Understanding the invasion, ecological adaptations, and management strategies of *Bactrocera dorsalis* in China: A review. *Horticulturae* **2023**, *9*, 1004. [\[CrossRef\]](#)
4. Wang, Y.H.; Wee, S.L.; De Faveri, S.; Gagic, V.; Hossain, S.; Cheng, D.F.; Chouangthavy, B.; Han, P.; Jiang, H.B.; Krutmuang, P.; et al. Advancements in integrated pest management strategies for *Bactrocera dorsalis* in Asia: Current status, insights, and future prospects. *Entomol. Gen.* **2024**, *44*, 1091–1116. [\[CrossRef\]](#)
5. Zeng, Y.; Reddy, G.V.P.; Li, Z.; Qin, Y.; Wang, Y.; Pan, X.; Jiang, F.; Gao, F.; Zhao, Z.H. Global distribution and invasion pattern of oriental fruit fly, *Bactrocera dorsalis* (Diptera: Tephritidae). *J. Appl. Entomol.* **2019**, *143*, 165–176. [\[CrossRef\]](#)
6. Li, X.L.; Li, D.D.; Cai, X.Y.; Cheng, D.F.; Lu, Y. Reproductive behavior of fruit flies: Courtship, mating, and oviposition. *Pest Manag. Sci.* **2024**, *80*, 935–952. [\[CrossRef\]](#)
7. Meng, L.W.; Yuan, G.R.; Lu, X.P.; Jing, T.X.; Zheng, L.S.; Yong, H.X.; Wang, J.J. Two delta class glutathione S-transferases involved in the detoxification of malathion in *Bactrocera dorsalis* (Hendel). *Pest Manag. Sci.* **2019**, *75*, 1527–1538. [\[CrossRef\]](#)
8. Chailleux, A.; Thiao, D.S.; Diop, S.; Bouvery, F.; Ahmad, S.; Caceres-Barrios, C.; Faye, E.; Brévault, T.; Diatta, P. Understanding *Bactrocera dorsalis* trapping to calibrate area-wide management. *J. Appl. Entomol.* **2021**, *145*, 831–840. [\[CrossRef\]](#)
9. Liu, H.; Wang, D.D.; Wan, L.; Hu, Z.Y.; He, T.T.; Wang, J.B.; Deng, S.Z.; Wang, X.S. Assessment of attractancy and safeness of (E)-coniferyl alcohol for management of female adults of oriental fruit fly, *Bactrocera dorsalis* (Hendel). *Pest Manag. Sci.* **2022**, *78*, 1018–1028. [\[CrossRef\]](#)
10. Wang, L.; Tian, S.H.; Zhao, W.; Wang, J.J.; Wei, D.D. Overexpression of ABCB transporter genes confer multiple insecticide tolerances in *Bactrocera dorsalis* (Hendel) (Diptera: Tephritidae). *Pestic. Biochem. Physiol.* **2023**, *197*, 105690. [\[CrossRef\]](#)
11. Chen, M.L.; Zhang, S.X.; Guo, P.Y.; Qin, Q.S.; Meng, L.W.; Yuan, G.R.; Wang, J.J. Identification and characterization of UDP-glycosyltransferase genes and the potential role in response to insecticides exposure in *Bactrocera dorsalis*. *Pest Manag. Sci.* **2023**, *79*, 666–677. [\[CrossRef\]](#) [\[PubMed\]](#)
12. Li, Z.; Chen, M.; Bai, W.; Zhang, S.; Meng, L.; Dou, W.; Wang, J.; Yuan, G. Identification, expression profiles and involvement in insecticides tolerance and detoxification of carboxylesterase genes in *Bactrocera dorsalis*. *Pestic. Biochem. Physiol.* **2023**, *193*, 105443. [\[CrossRef\]](#)
13. Liao, M.S.; Chuang, C.L.; Lin, T.S.; Chen, C.P.; Zheng, X.Y.; Chen, P.T.; Liao, K.C.; Jiang, J.A. Development of an autonomous early warning system for *Bactrocera dorsalis* (Hendel) outbreaks in remote fruit orchards. *Comput. Electron. Agric.* **2012**, *88*, 1–12. [\[CrossRef\]](#)
14. Li, X.Z.; Wang, G.L.; Wang, C.L.; Li, W.J.; Lu, T.; Ge, Y.G.; Xu, C.K.; Zhong, X.; Wang, J.G.; Yang, H.Y. Long-term monitoring of *Bactrocera* and *Zeugodacus* spp. (Diptera: Tephritidae) in China and evaluation of different control methods for *Bactrocera dorsalis* (Hendel). *Crop Prot.* **2024**, *182*, 106708. [\[CrossRef\]](#)
15. Guo, Q.; Wang, C.; Xiao, D.; Huang, Q. Automatic monitoring of flying vegetable insect pests using an RGB camera and YOLO-SIP detector. *Precis. Agric.* **2023**, *24*, 436–457. [\[CrossRef\]](#)
16. Čirjak, D.; Miklečić, I.; Lemić, D.; Kos, T.; Pajač Živković, I. Automatic pest monitoring systems in apple production under changing climatic conditions. *Horticulturae* **2022**, *8*, 520. [\[CrossRef\]](#)
17. Fan, Y.; Zhang, C.; Qin, Y.; Yin, X.; Dong, X.; Desneux, N.; Zhou, H. Monitoring the methyl eugenol response and non-responsiveness mechanisms in oriental fruit fly *Bactrocera dorsalis* in China. *Insects* **2022**, *13*, 1004. [\[CrossRef\]](#)
18. Ding, W.; Taylor, G. Automatic moth detection from trap images for pest management. *Comput. Electron. Agric.* **2016**, *123*, 17–28. [\[CrossRef\]](#)
19. Fukatsu, T.; Watanabe, T.; Hu, H.; Yoichi, H.; Hirafuji, M. Field monitoring support system for the occurrence of *Leptocoris chinensis* Dallas (Hemiptera: Alydidae) using synthetic attractants, field servers, and image analysis. *Comput. Electron. Agric.* **2012**, *80*, 8–16. [\[CrossRef\]](#)
20. Jiang, J.A.; Tseng, C.L.; Lu, F.M.; Yang, E.C.; Wu, Z.S.; Chen, C.P.; Lin, S.H.; Lin, K.C.; Liao, C.S. A GSM-based remote wireless automatic monitoring system for field information: A case study for ecological monitoring of the oriental fruit fly, *Bactrocera dorsalis* (Hendel). *Comput. Electron. Agric.* **2008**, *62*, 243–259. [\[CrossRef\]](#)

21. Tariq, S.; Hakim, A.; Siddiqi, A.A.; Owais, M. An image dataset of fruit fly species (*Bactrocera zonata* and *Bactrocera dorsalis*) and automated species classification through object detection. *Data Brief* **2022**, *43*, 108366. [CrossRef] [PubMed]
22. Diller, Y.; Shamsian, A.; Shaked, B.; Altman, Y.; Danziger, B.C.; Manrakhan, A.; Serfontein, L.; Bali, E.; Wernicke, M.; Egartner, A.; et al. A real-time remote surveillance system for fruit flies of economic importance: Sensitivity and image analysis. *J. Pest Sci.* **2023**, *96*, 611–622. [CrossRef]
23. Kamilaris, A.; Prenafeta-Boldú, F.X. Deep learning in agriculture: A survey. *Comput. Electron. Agric.* **2018**, *147*, 70–90. [CrossRef]
24. Buslaev, A.; Iglovikov, V.I.; Khvedchenya, E.; Parinov, A.; Druzhinin, M.; Kalinin, A.A. Albumentations: Fast and flexible image augmentations. *Information* **2020**, *11*, 125. [CrossRef]
25. Qiu, R.Z.; Chen, S.P.; Chi, M.X.; Wang, R.B.; Huang, T.; Fan, G.C.; Zhao, J.; Weng, Q.Y. An automatic identification system for citrus greening disease (huanglongbing) using a YOLO convolutional neural network. *Front. Plant Sci.* **2022**, *13*, 1002606. [CrossRef]
26. O’Shea-Wheller, T.A.; Corbett, A.; Osborne, J.L.; Recker, M.; Kennedy, P.J. VespaAI: A deep learning-based system for the detection of invasive hornets. *Commun. Biol.* **2024**, *7*, 354. [CrossRef] [PubMed]
27. Xiong, B.; Li, D.; Zhang, Q.; Desneux, N.; Luo, C.; Hu, Z. Image detection model construction of *Apolygus lucorum* and *Emoiasca* spp. based on improved YOLOv5. *Pest Manag. Sci.* **2024**, *80*, 2577–2586. [CrossRef]
28. Wang, N.; Fu, S.; Rao, Q.; Zhang, G.; Ding, M. Insect-YOLO: A new method of crop insect detection. *Comput. Electron. Agric.* **2025**, *232*, 110085. [CrossRef]
29. Zhang, W.; Huang, H.; Sun, Y.; Wu, X. AgriPest-YOLO: A rapid light-trap agricultural pest detection method based on deep learning. *Front. Plant Sci.* **2022**, *13*, 1079384. [CrossRef]
30. Wen, C.; Chen, H.; Ma, Z.; Zhang, T.; Yang, C.; Su, H.; Chen, H. Pest-YOLO: A model for large-scale multi-class dense and tiny pest detection and counting. *Front. Plant Sci.* **2022**, *13*, 973985. [CrossRef] [PubMed]
31. Sohan, M.; Sai Ram, T.; Rami Reddy, C.V. A review on YOLOv8 and its advancements. In Proceedings of the International Conference on Data Intelligence and Cognitive Informatics, Tirunelveli, India, 18–20 November 2024; pp. 529–545.
32. Hossin, M.; Sulaiman, M.N. A review on evaluation metrics for data classification evaluations. *Int. J. Data Min. Knowl. Manag. Process* **2015**, *5*, 1–11.
33. Preti, M.; Verheggen, F.; Angeli, S. Insect pest monitoring with camera-equipped traps: Strengths and limitations. *J. Pest Sci.* **2021**, *94*, 203–217. [CrossRef]
34. Sun, D.; Zhang, K.; Zhong, H.; Xie, J.; Xue, X.; Yan, M.; Wu, W.; Li, J. Efficient tobacco pest detection in complex environments using an enhanced YOLOv8 model. *Agriculture* **2024**, *14*, 353. [CrossRef]
35. Yin, J.; Huang, P.; Xiao, D.; Zhang, B. A lightweight rice pest detection algorithm using improved attention mechanism and YOLOv8. *Agriculture* **2024**, *14*, 1052. [CrossRef]
36. Sun, Y.; Liu, X.; Yuan, M.; Ren, L.; Wang, J.; Chen, Z. Automatic in-trap pest detection using deep learning for pheromone-based *Dendroctonus valens* monitoring. *Biosyst. Eng.* **2018**, *176*, 140–150. [CrossRef]
37. Roosjen, P.P.J.; Kellenberger, B.; Kooistra, L.; Green, D.R.; Fahrelnatrapp, J. Deep learning for automated detection of *Drosophila suzukii*: Potential for UAV-based monitoring. *Pest Manag. Sci.* **2020**, *76*, 2994–3002. [CrossRef]
38. Dai, F.; Wang, F.; Yang, D.; Lin, S.; Chen, X.; Lan, Y.; Deng, X. Detection method of citrus psyllids with field high-definition camera based on improved cascade region-based convolution neural networks. *Front. Plant Sci.* **2022**, *12*, 816272. [CrossRef]
39. Wang, J.; Wang, J. A lightweight YOLOv8 based on attention mechanism for mango pest and disease detection. *J. Real-Time Image Process* **2024**, *21*, 136. [CrossRef]
40. Wang, X.; Xiao, T.; Jiang, Y.; Shao, S.; Sun, J.; Shen, C. Repulsion loss: Detecting pedestrians in a crowd. In Proceedings of the IEEE Conference on Computer Vision and Pattern Recognition, Salt Lake City, UT, USA, 18–23 June 2018; pp. 7774–7783.
41. Ghiasi, G.; Cui, Y.; Srinivas, A.; Qian, R.; Lin, T.Y.; Cubuk, E.D.; Le, Q.V.; Zoph, B. Simple copy-paste is a strong data augmentation method for instance segmentation. In Proceedings of the IEEE/CVF Conference on Computer Vision and Pattern Recognition, Nashville, TN, USA, 20–25 June 2021; pp. 2918–2928.

Disclaimer/Publisher’s Note: The statements, opinions and data contained in all publications are solely those of the individual author(s) and contributor(s) and not of MDPI and/or the editor(s). MDPI and/or the editor(s) disclaim responsibility for any injury to people or property resulting from any ideas, methods, instructions or products referred to in the content.